

Radiation growth of *hcp* crystals driven by discrete breathers

V.I. Dubinko

vdubinko@mail.ru

NSC Kharkov Institute of Physics and Technology, 61108, Kharkov, Ukraine

A new mechanism of radiation growth (RG) of hexagonal close pack (*hcp*) crystals is proposed, which is based on the radiation-induced creation of moving 'discrete breathers' (DBs), *i.e.* large amplitude anharmonic lattice vibrations, which can propagate and transfer energy along close-packed crystallographic directions within the basal planes of and excite atoms at prismatic faces/edges. Accordingly, the DB-induced vacancy emission from prismatic faces is enhanced as compared to that from the basal faces, at which only thermally activated vacancy emission takes place. This should result in the vacancy diffusional flow from prismatic to basal faces leading to expansion along the **a**-directions and to contraction along the **c**-axis, *i.e.* to the radiation-induced growth. The RG rate driven by this mechanism is evaluated in the framework of a rate theory modified with account of the DB-induced vacancy emission.

Keywords: moving discrete breathers, anisotropic vacancy emission, radiation growth.

1. Introduction

The radiation growth (RG) of Zr-based materials is one of the main concerns for the safe operation of thermal nuclear reactors. More generally, RG is the name given to the volume-conserved shape deformation that occurs in non-cubic crystalline materials under irradiation in the absence of an applied stress [1–5]. The best-known examples of irradiation growth are found in *hcp* metals — graphite, uranium, zirconium and its alloys (see [1–3] for the review). In most cases, RG corresponds to an expansion along the **a**-direction and a contraction along the **c**-direction in its constituent grains [1]. Available models of RG are based on the anisotropy of migration of point defects (usually, self-interstitial atoms — SIAs) produced by irradiation [4] or mobile SIA-clusters produced by cascade damage [4,5]. However, recent *ab-initio* results [6] indicate that the ratio of diffusion coefficients parallel and perpendicular to the basal planes is higher for vacancies as compared to SIA at temperatures below 600 K. This raises doubts that the observed radiation growth in Zr irradiated with 1 MeV electrons, namely positive strains in prismatic and negative strains in basal directions, and void alignment along basal planes [7], can be explained by the anisotropy of point defect diffusion, which predicts opposite strain signs. Electron irradiation does not produce cascades, and hence, in-cascade SIA-clusters cannot explain these effects as well, since a homogeneous nucleation of SIA-clusters is completely negligible. So, it becomes evident that the mechanisms involved in the irradiation growth of *hcp* metals may be more complicated than those considered within the conventional rate theory models.

In this paper, we propose a principally new RG mechanism based on the radiation-induced creation of 'discrete breathers' (DBs), *i.e.* spatially localized large-amplitude vibrational

modes in lattices that exhibit strong anharmonicity. DBs in real crystals radiate energy very slowly because their main vibrational frequency lies outside the phonon band. They have been successfully observed experimentally in various physical systems [8,9]. Studies of the DBs in three-dimensional crystals by means of molecular dynamics (MD) simulations using realistic interatomic potentials include ionic crystals with NaCl structure [10], graphene [11], semiconductors [12] and metals [13–19]. Semiconductors and metals possess no gap in phonon spectrum and thus DBs may exist only if their frequency is positioned above the phonon spectrum. Such high frequency DBs may be stable due to the screening of the short-range ion — ion interaction by the conducting electrons as was argued and demonstrated by Hizhnyakov et al [13–15]. Namely, MD simulations of lattice excitation in *fcc* nickel as well as in *bcc* niobium and iron using realistic many-body interatomic potentials have proven that stable high-frequency DBs exist in these metals. Notably, the threshold DB energy is relatively small (fractions of eV) as compared to the formation energy of a stable Frenkel pair in those metals (several eV). Moreover, it has been shown that DBs in metals are highly mobile, hence can efficiently transfer a concentrated vibrational energy over large distances along close-packed crystallographic directions [15–20]. Recently, a theoretical background has been proposed to ascribe the interaction of moving DBs (also termed quodons [23]) with lattice defects to rationalize various radiation-induced phenomena, such as irradiation creep [21], swelling [22], void lattice formation [23], radiation-induced softening [24]. The underlying mechanisms of these phenomena are based on the enhancement of emission of point defects from extended defects — dislocations, voids, grain boundaries and precipitates [22,25,26]. RG is another technologically important example of such phenomena.

As demonstrated in the present article, RG of *hcp* metals

can be related to the natural anisotropy of DB propagation in *hcp* metals, where all six close-packed directions lie within the basal plane [19].

The paper is organized as follows. In the next section, salient point of RG in *hcp* metals are briefly discussed along with current theoretical models for its description. In section 3, recent MD results on the DB properties in *bcc* and *hcp* metals are presented. In section 4, a rate theory model of the RG is proposed based on anisotropy of DB propagation in *hcp* crystals. Radiation-induced production of DBs is considered in section 5. The results are summarized in section 6.

2. Previous models of radiation growth

Irradiation growth in *hcp* zirconium was first observed in single crystals about 50 years ago. Since then, experiments consistently showed that irradiation growth in polycrystalline zirconium and its single-phase alloys roughly correspond to an expansion along the *a*-direction and a contraction along the *c*-direction [1] (Fig.1). Irradiation growth measurements for zirconium and its alloys have been performed mainly in the temperature ranges 50–80 °C, 280–400 °C, and 400–450°C, which are usually referred to as the low, medium and high temperature growth regimes. Low temperature irradiation-damage annealing studies indicate that at temperatures below 400 K, vacancies in Zircaloy are not mobile [4]. So the first two regimes should be related to diffusion anisotropy difference (DAD) of self-interstitial atoms (SIAs), unless vacancy diffusion is facilitated by some impurity atoms such as Fe [4]. High temperature RG has been attributed mainly to the production of SIA clusters in displacement cascades, which perform 1-D diffusion along close-packed directions within the basal plane. These models [4–6] are similar to production bias models (PBM) developed to describe the void swelling in cubic metals. However, as has been demonstrated in Ref.[22], the PBM pretense at quantitative description of the void swelling under cascade damage is not validated by experimental data, while under electron damage, the PBM cannot be used at all. Similarly, in-cascade SIA-clusters cannot be applied to the RG explanation under electron irradiation. On the other hand, DAD mechanisms are also challenged by recent ab-initio modeling [6] indicating that the ratio of diffusion coefficients parallel and perpendicular to the basal planes

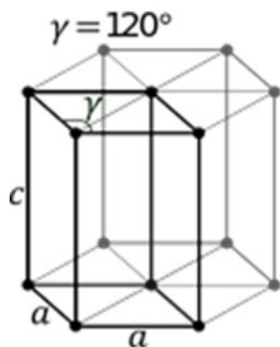


Fig. 1. Sketch of the unit cell of a *hcp* crystal, in which there are 6 close-packed directions lying in the basal plane perpendicular to the *c*-direction.

is higher for vacancies as compared to SIA at temperatures below 600 K, which should result in the RG along the *c*-axis, contrary to the experimental observations. So, it becomes evident that the explanation of RG should be extended beyond the conventional rate theory models, which will be attempted in the next sections.

3. Discrete breathers in metals

For a long time it has been assumed that the softening of atomic bonds with increasing vibrational amplitude is a general property of crystals, and therefore DS's with frequencies above the top phonon frequency cannot occur. However, recently Haas et al [13] have provided a new insight into this problem by demonstrating that the anharmonicity of metals appears to be very different from that of insulators. The point is that the essential contribution to the screening of the atomic interactions in metals comes from free electrons at the Fermi surface. As a consequence, the ion-ion attractive force may acquire a nonmonotonic dependence on the atomic distance and may be enhanced resulting in an amplification of even anharmonicities for the resulting two-body potentials. This effect can counteract the underlying softening associated with the bare potentials with a moderate increase of vibrational amplitudes to permit the existence of DS's above the top of the phonon spectrum. As a result, in some metals, DS's may exist with frequencies above the top of the phonon spectrum. Below we consider two relevant examples, namely, *bcc* Fe, where the most comprehensive studies of the DB interaction with crystal defects have been made [18] and *hcp* Zr [19], for which RG presents the most urgent technological problem.

3.1. DBs in *bcc* Fe

The behavior of standing and moving DBs has been studied by Terentyev et al [18] by classical MD simulations in 3D periodic *bcc* Fe using well spread interatomic potentials (IAPs). MD simulations were done in the virtual 3D-periodic crystals with three principal axes *x*, *y* and *z* oriented along the $\langle 111 \rangle$, $\langle -12-1 \rangle$ and $\langle -101 \rangle$ directions, respectively. A DB was created in the crystal by providing initial displacement along *x* direction to six neighboring atoms selected in the center following the procedure [13], the key feature of which is the initial displacement of the two adjacent atoms from their equilibrium position along the close $\langle 111 \rangle$ direction, which should oscillate in the *anti-phase mode* with respect to each other thus forming a stable DB. The initial offset displacement d_0 determines the DB amplitude and oscillation frequency and, ultimately, its lifetime. DBs can be excited in a narrow frequency band $(1 \div 1.4) \times 10^{13} \text{ s}^{-1}$ just above the Debye frequency of *bcc* Fe, and DB frequency grows with increasing amplitude as expected from the «hard» type anharmonicity of the considered vibrational mode. Application of a displacement larger than 0.45 Å generates a chain of *focusons*, while a displacement smaller than 0.27 Å does not provide enough potential energy for the two oscillators to initiate a stable DB and the atomic oscillations decay quickly by losing its energy to *phonons*.

The movement of a DB can be induced by translational kinetic energy E_{tr} given to the two central DB atoms along close-packed direction (111). Their velocities range from about 300 to 2000 m/s while travel distances range from several dozens to several hundreds of atomic spaces, depending on the d_0 and E_{tr} [18]. Figure 2a shows a DB approaching the atoms with index 3415 and 3416. The two atoms pulsate in the anti-phase mode for about 1ps (~10 oscillations) and then oscillations cease but they are resumed at the subsequent atoms along the x-axis. In this way, the DB moves at a speed of 2.14 km/s, *i.e.* about the half speed of sound in *bcc* Fe. The translational kinetic energy of the DB is about 0.54 eV, which is shared among two core atoms, giving 0.27 eV per atom. This is very close to the initial kinetic energy $E_{tr}=0.3$ eV transmitted to the atoms to initiate the DB movement. The deviation of the potential energy of the atoms from the ground state during the passage of the DB is presented in Fig.2b. The amplitude of the energy deviation can reach almost 1 eV. In an oversimplified ‘thermodynamic’ analogy, a moving DB can be viewed as an atom-size spot heated above 10000 K propagating through the crystal at sub-sonic speed.

If a moving DB encounters on its way a crystal defect such as a vacancy, free surface or a dislocation, it excites the nearby atoms, the energy of which deviates from the ground state. The oscillation of the potential energy of a surface atom hit by the DB is shown in Fig.3, against the one obtained for

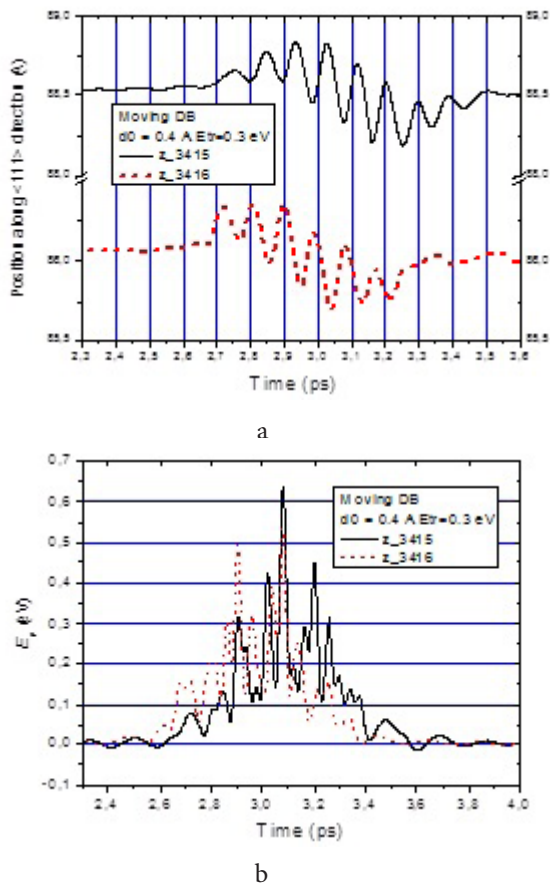


Fig. 2. Oscillation of x coordinate of two neighbouring atoms, 3415 and 3416 in a [111] row in Fe during the passage of a moving DB ($d_0 = 0.4$ Å, $E_{tr} = 0.3$ eV); (b) deviation of the potential energy of the atoms from the ground state during the passage of a DB [18].

a frontal vacancy atom. The energy oscillation of the surface atom is essentially higher than that for the near-vacancy atoms. Fig.4 shows the scattering of a DB on the core of an edge dislocation. Apparently, only the frontally hit atom 'B' exhibits essential vibration. The integral under the curve for the atom B is 0.15 eV, which is comparable with that for the near-vacancy atom A. The dislocation excitation time is about 2 ps ~20 atomic oscillation periods, which is close to the excitation time for DB-vacancy or DB-free surface interaction.

Note that DB excitations and scattering on the defects presented in Figs.2—4, were done in conditions imitating a periodic perfect crystal at zero temperature, *i.e.* when all other atoms were initially at their lattice positions and had zero initial velocities.

3.2. DBs in hcp Zr

MD modeling of moving DBs in Zr has been done by Kistanov and Murzaev [19] using LAMMPS and imbedded IAPs. The computational cell size was $30 \times 10 \times 10$ atomic planes or 12000 atoms, and periodic boundary conditions were applied at constant volume and energy. DBs were excited within the basal planes along close-packed directions [1010]. To do so, atoms in the close-packed array (highlighted in Fig.5) were

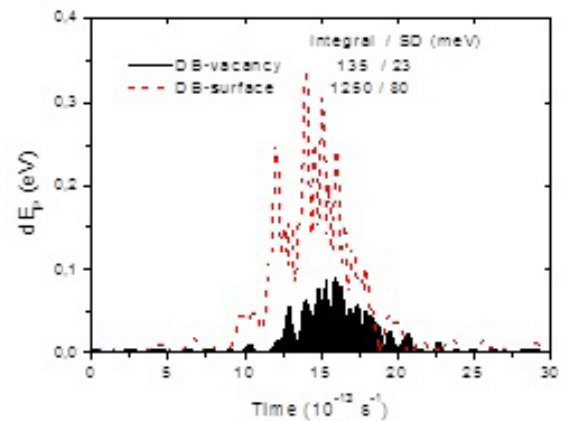


Fig. 3. Energy deviation from the ground state vs. time for a frontal vacancy atom and an atom at the free surface due to their interaction with a DB ($d_0 = 0.4$ Å, $E_{tr} = 0.3$ eV) [18]. Integral and standard deviation (SD) of energy are also shown.

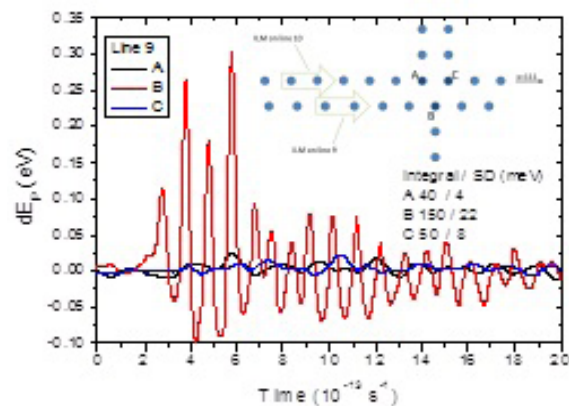


Fig. 4. Variation of the potential energy of atoms surrounding a core of $\frac{1}{2}\langle 111 \rangle \langle 110 \rangle$ edge dislocation caused by the scattering of the DB ($d_0 = 0.4$ Å, $E_{tr} = 0.3$ eV) moving along the 'Line 9' [18].

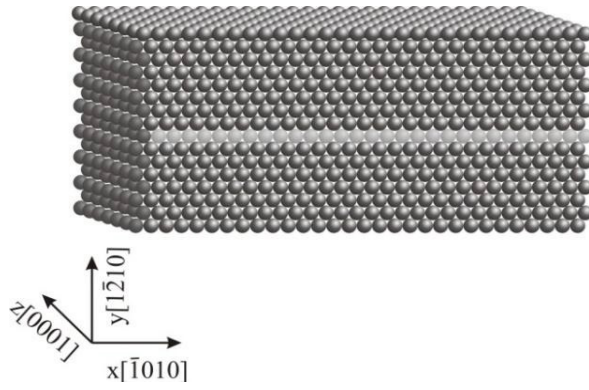


Fig. 5. The computational cell. To excite a moving DB, atoms in the close-packed array (highlighted) were given initial displacements and velocities according to the ansatz [20]. All other atoms were initially at their lattice positions and had zero initial velocities.

given initial displacements and velocities according to the ansatz [20].

DB parameters include frequency, ω , velocity, V , oscillation amplitude, A , amplitude of deviations of atom centers, B , the phase difference of oscillation of adjacent atoms, δ , which determines the DB velocity (for $\delta=0$, one has a standing DB) and DB localization parameters, β , γ . Fig.6 shows dependence of the DB frequency on the oscillation amplitude and DB velocity V on the phase difference δ .

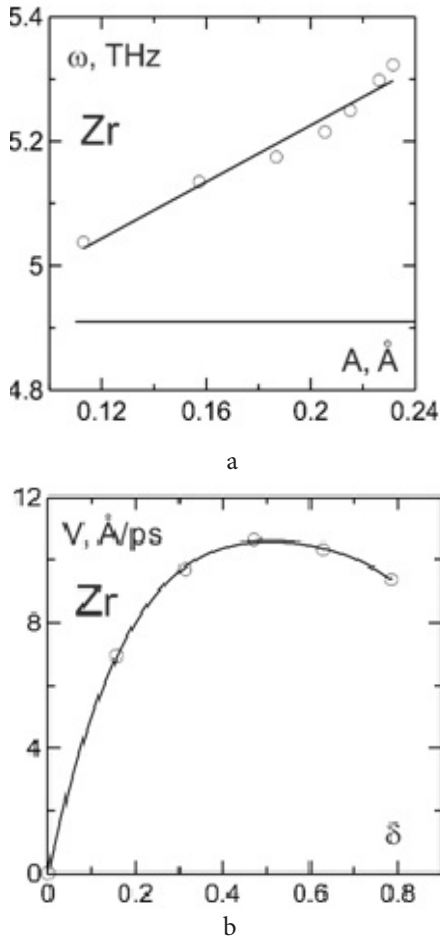


Fig. 6. Dependence of the DB frequency on amplitude (at $A = 0.2 - 0.5$, $B = 0.016$, $\beta = 0.7$, $\gamma = 0.8$) and velocity on the phase difference δ (at $A = 0.4$, $B = 0.016$, $\beta = 0.7$, $\gamma = 0.8$) [19].

It can be seen that the DB frequency lies above the maximum phonon frequency (shown with horizontal line in Fig.6), and its maximum velocity is about 1000 m/s which is about 22% of the sound velocity of Zr. Similar results have been obtained for *hcp* Be, Mg and Ti [19].

4. Breather-induced mechanism of RG

Due to the natural anisotropy of Zr, all six close-packed directions lie within the basal plane. Accordingly, all the grain boundaries (GBs) perpendicular to the basal plane act as the scattering places for moving DBs produced in the bulk by irradiation (see the next section). On the other hand, GBs parallel to the basal plane do not interact with moving DBs. Due to this anisotropy, the rate of the vacancy emission from GBs perpendicular to the basal plane (GBper) can be higher than that from GBs parallel to the basal plane (GBpar), and this difference should depend on the DB flux to GBper. The point is that when a DB is scattered at the GBper, it excites an atom at the scattering site (see Fig.3), which should result in the oscillation of the energy barrier for this atom to leave the regular position and become an adatom. These oscillations take the time τ_{ex} , during which they have been shown to amplify the rate of thermally activated formation of adatom. The amplification factor is close to $I_0(\epsilon_{ex}^f/k_B T)$, where $I_0(x)$ is the zero order, modified Bessel function of x of the first kind, ϵ_{ex} is the energy excitation amplitude, k_B is the Boltzmann constant and T is the lattice temperature [24]¹.

A vacant site appeared in the process of the adatom creation can be subsequently filled either by adatom itself (recombination) or by another nearby atom, including the atoms from the second (from the surface) atomic layer. In the latter case, a vacancy formed at the surface diffuses to the bulk, and this is a classical Schottky mechanism of formation of vacancies (Schottky defects) in crystals [21]. We are concerned here with the acceleration of this process due to the interaction of the surface with moving DBs produced in the bulk by irradiation. As a result of this acceleration, the local equilibrium concentration of vacancies at GB^{per} will be increased and given by the following expression²:

$$C_v^{DB} = C_v^{th} \left(1 + I_0 \left(\frac{\epsilon_{ex}^f}{k_B T} \right) \omega_{ex} \tau_{ex} \right), \quad (1)$$

where $C_v^{th} = \exp(-E_v^f/k_B T)$ is the thermal equilibrium concentration of vacancies, E_v^f is the vacancy formation energy, ω_{ex} is the mean number of excitations per surface atom per second caused by DBs, which is proportional to the DB flux Φ_{DB} and the cross-section of DB-atom interaction ($\sim a \times c$, where a and c are the lattice parameters) and is given by

$$\omega_{ex} = \Phi_{DB} ac, \quad \Phi_{DB} = C_{DB} V_{DB} / v_a, \quad (2)$$

¹ A more detailed study of the periodically driven stochastic systems shows that the amplification factor depends also on the barrier height, E_b , but this dependence is weak for $E \ll E_b$ [27].

² Derivation of Eq.(1) is similar to that described in details in Ref.[22] for ballistic mechanism of vacancy production by energetic DBs with $\epsilon_{ex}^f > E_v^f$.

where C_{DB} is the mean DB concentration (per atom) in the bulk, which depends on the rate of *radiation-induced production of DBs*, i.e. on irradiation flux (see the next section), V_{DB} is the mean DB velocity and v_a is the atomic volume.

On the other side, the local equilibrium concentration of vacancies at GB^{par} will be unaffected by DBs and equal to its thermal equilibrium value C_v^{th} . As a result, a net flux of vacancies from GB^{per} to GB^{par} will arise, which will lead to the contraction along *c*-axis and elongation along *a*-directions, i.e. to the RG at a rate given by equation similar to the Nabarro-Herring equation for the diffusion creep under applied stress [28]

$$\frac{d\varepsilon}{dt} = \frac{D_v^{DB}}{d^2} (C_v^{DB} - C_v^{th}), \quad D_v^{th} = D_v^0 \exp\left(-\frac{E_v^m}{k_b T}\right), \quad (3)$$

$$D_v^{DB} = D_v^{th} \left(1 + I_0 \left(\frac{\varepsilon_{ex}^m}{k_b T} \right) \omega_{ex} \tau_{ex} \right), \quad (4)$$

where E_v^m is the vacancy migration energy, d is the mean grain size, and D_v^{DB} is the radiation-enhanced vacancy diffusion coefficient due to their interactions with DBs. The vacancy migration enhancement has the form similar to that of formation given by Eq.(1), with the only significant difference in the excitation amplitudes, being higher for the surface atoms than for the vacancy atoms: $\varepsilon_{ex}^f > \varepsilon_{ex}^m$ (Fig.3).

The main difference of the proposed mechanism from Nabarro-Herring mechanism is that in the latter case, the vacancy concentration difference was induced by applied stress, while in the case under consideration, it is induced by the anisotropy of DB propagation in *hcp* crystals.

Substituting Eq.(1) in Eq.(3) one obtains the following equation for the RG rate

$$\frac{d\varepsilon}{dt} = \frac{D_v^{DB} C_v^{th}}{d^2} I_0 \left(\frac{\varepsilon_{ex}^f}{k_b T} \right) \omega_{ex} \tau_{ex}. \quad (5)$$

In order to express the RG rate via irradiation flux one need to consider kinetics of DB excitation under irradiation, which will be done in the following section.

5. Excitation of DBs under irradiation

The rate equation for the concentration of DBs with energy E , $C_{DB}(E, t)$ can be written as follows [24]

$$\frac{\partial C_{DB}(E, t)}{\partial t} = K_{DB}(E) - \frac{C_{DB}(E, t)}{\tau_{DB}(E)}, \quad (6)$$

where $K_{DB}(E)$ is the rate of creation of DBs with energy $E > E_{min}$ and $\tau_{DB}(E)$ is the DB lifetime. It has an obvious steady-state solution ($\partial C_{DB}(E, t)/\partial t = 0$):

$$C_{DB}(E) = K_{DB}(E) \tau_{DB}(E), \quad (7)$$

Moving DBs are expected to arise only under irradiation with energetic particles (electrons, ions or neutrons), which can give lattice atoms not only energy but also impulse required to initiate their propagation along one of

the close-packed directions. In the MD simulations [19], this corresponds to non-zero phase shift $\delta \neq 0$, whereas thermal equilibrium corresponds to the case $\delta = 0$, in which only standing DBs are expected to arise due to thermal fluctuations [24,27].

Under irradiation, DBs *may be the transient form of the heat generation*, as it has been argued in Refs.[25,26], which means that they are constantly generated by irradiation, and subsequently lose energy by generating phonons, whence it follows that the mean DB production rate can be evaluated using simple energy considerations as follows.

Let K_{DB} be the average rate of DB generation (per atomic site per second), which should be proportional to the flux of impinging particles, F_{irr} , and the energy deposition density by one particle, dE_{irr}/dx , and inversely proportional to the mean DB energy [26]

$$K_{DB} = k_{eff} F_{irr} \left(\frac{dE_{irr}}{dx} \right) \frac{v_a}{E_{DB}}, \quad (8)$$

where F_{irr} is the flux of impinging particles, which lose their energy by producing DBs of the mean energy E_{DB} , k_{eff} is the DB production efficiency that depends on material and irradiation conditions and can range from zero (no DB generation) to unity (e.g. under sub-threshold irradiation that does not produce stable defects). Noting that the mean DB lifetime is given by $\tau_{DB} = l_{DB}/V_{DB}$, where l_{DB} is the mean DB propagation range, and substituting Eq.(7) into (2), one obtains the following equation for the surface atom excitation frequency via the irradiation flux

$$\omega_{ex} = K_{DB} \frac{acl_{DB}}{v_a} = K_{dpa} k_{dpa}^{DB} \frac{acl_{DB}}{v_a}, \quad (9)$$

where K_{dpa} is the production rate of displacements per atom (dpa), and k_{dpa}^{DB} is rate of DB production per dpa, which is about 10^6 for 1 MeV electron irradiation at $k_{eff} = 1$ [26].

Substituting Eq.(9) in (5) one obtains the RG rate per dpa expressed via DB parameters deduced from MD simulations and listed in Table 1:

Table 1.

Material parameters used in calculations

Lattice parameter, a (nm)	0.323 [4]
Lattice parameter, c (nm)	0.5147 [4]
Atomic volume, v_a (nm ³)	0.0236 [1]
Vacancy formation energy, E_v^f (eV)	1.6 [1]
Vacancy migration energy, E_v^m (eV)	1.3 [1]
Vacancy diffusivity factor, D_v^0 (m ² s ⁻¹)	2.6×10^{-5}
DB production efficiency, k_{eff}	1 [26]
Mean DB energy, E_{DB} (eV)	1 [26]
Mean DB range, l_{DB} (nm)	1000
Surface excitation energy, ε_{ex}^f (eV)	0.8
Vacancy excitation energy, ε_{ex}^m (eV)	0.3
Mean excitation time, τ_{ex} (ps)	2
DB to FP production ratio, k_{FP}^{DB}	10^6 [26]

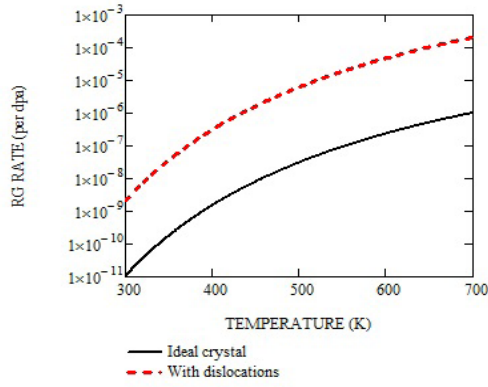


Fig. 7. RG rate vs. temperature for ideal crystal, $\rho_d = 0$, Eq.(10) and for $\rho_d = 10^{14} \text{ m}^{-2}$, Eq.(11). $d = 1$ micron.

$$\frac{d\varepsilon}{d(dpa)} = \frac{D_v^{DB} C_v^{th}}{d^2} I_0 \left(\frac{\varepsilon_{ex}^f}{k_b T} \right) \tau_{ex} k_{dpa}^{DB} \frac{acl_{DB}}{\nu_a}. \quad (10)$$

Equation (10) describes RG in ideal crystal with no dislocations, in which case its temperature dependence is shown in Fig.7 (solid curve).

However, in real crystals, dislocations play a crucial role in RG [1–7], and they can be taken into account in the present model by assuming that dislocations with a-component Burgers vectors (a-dislocations) interact with DBs moving along a-directions (as in the case shown in Fig.4) stronger than those with c-component Burgers vectors (c-dislocations). Accordingly, c-dislocations will act as effective sinks for vacancies emitted from GBs and a-dislocations, which will result in the following modification of Eq.(10):

$$\frac{d\varepsilon}{d(dpa)} = D_v^{DB} C_v^{th} (k_{GB}^2 + k_d^2) I_0 \left(\frac{\varepsilon_{ex}^f}{k_b T} \right) \tau_{ex} k_{dpa}^{DB} \frac{acl_{DB}}{\nu_a} \quad (11)$$

$$k_{GB}^2 \approx \frac{1}{d^2}, \quad k_d^2 \approx 2\rho_d,$$

where k_{GB}^2 is the GB sink strength, k_d^2 is the dislocation sink strength [22] and ρ_d is the dislocation density.

As can be seen from Fig.7,8 the RG rate increases with increasing temperature, dislocation density and with decreasing grain size. All these trends are confirmed by experimental data [1–3].

Note that dose rate enters in the expression for the radiation-induced diffusion (4), but its evaluation shows that the effect becomes significant only below 200 K. That is why the RG rate predicted by the model practically does not depend on the dose rate (or neutron flux), which also agrees with experimental data [3]: “Judging by the results on similar materials after irradiation in different reactors with fluxes ranging from 1 to $20 \times 10^{17} \text{ nm}^{-2}\text{s}^{-1}$, the growth strain of a given material beyond the initial transients appears to be determined only by the test temperature and neutron fluence and is independent of the time to reach that fluence.”

5. Discussion and outlook

In the present paper, a new mechanism of radiation growth of *hcp* crystals was proposed, which is based on the

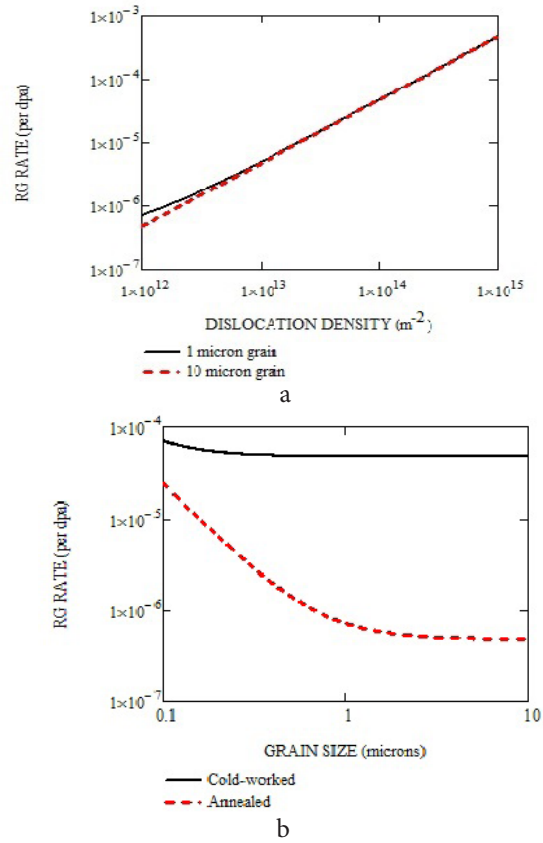


Fig. 8. RG rate vs. (a) dislocation density and (b) grain size at 600 K predicted by Eq.(11) at material parameters presented in Table 1. In the cold-worked/annealed state, $\rho_d = 10^{14} / 10^{12} \text{ m}^{-2}$, respectively.

radiation-induced creation of moving DBs that can transfer energy along close-packed crystallographic directions within the basal planes and excite atoms at prismatic faces/edges and at the cores of a-dislocations. Accordingly, the DB-induced vacancy emission from prismatic faces and a-dislocations is enhanced as compared to that from the basal faces and c-dislocations. This results in the vacancy diffusional flow from prismatic faces and a-dislocations to basal faces and c-dislocations leading to expansion along the a-directions and to contraction along the c-axis, *i.e.* to the experimentally observed RG. Based on the model, simple analytical equations for the RG rate were derived, which predict its increase with increasing temperature, dislocation density and with decreasing grain size. All these trends are confirmed by experimental data.

For a more detailed quantitative comparison between a theory and experiment one needs to include in the analysis also the fluxes of vacancies and SIAs produced by irradiation in the bulk. These fluxes affect the growth and shrinkage of a-type SIA and vacancy dislocation loops, which can coexist under irradiation due to the sophisticated dependence of the loop bias for SIA absorption on the loop size and sink strengths [29,30]. Another important microstructural component accompanying the so called break away growth is large vacancy c-loops formed at later irradiation stages, which is consistent with our assumption about their weaker interaction with DBs compared to that for a-loops.

Another peculiarity of radiation damage in *hcp* metals

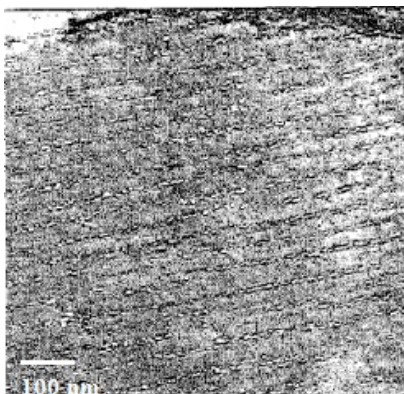


Fig. 9. Alignment of voids in bands parallel to the basal planes in electron-irradiated high purity Zr [31].

is the alignment of vacancy type defects, a-dislocation loops and voids, along the basal planes, which has been observed both under neutron and electron irradiation [7,31] (Fig.9).

This phenomena is similar to the 3-D void lattice formation in cubic metals [32], which has been explained as follows [23,33]. If the DB propagating range is larger than the void spacing, the voids can shield each other from DB fluxes along the close packed directions, and so, the vacancy emission rate for voids, which have more immediate neighbors along the close packed direction, becomes smaller than that for other voids, and they start to have some advantage in growth (Fig.10). Quantitatively, it means that C_v^{DB} for the “locally ordered” voids is lower than that for the locally “interstitial” voids. If the void number density is sufficiently high, the competition between them can be shown to make the “interstitial” voids shrink away resulting in the void lattice formation, in which the nearest neighbors are arranged along the close-packed directions of the host lattice. For cubic metals this means that the void lattice copes the host lattice, while in *hcp* metals, the alignment of voids or a-loops in bands parallel to the basal planes (in which DB propagate) is expected, in agreement with experimental data. This driving force for the void ordering was proposed by Dubinko [33] well before the existence of DB in metals was demonstrated. Subsequent results on the DB mobility in *bcc* and *hcp* metals strongly support this model, which is the only one that explains the ordering phenomena both under neutron and electron irradiation.

In conclusion, we note that DB excitations in refs [18,19] were modelled in a cell with initial and boundary conditions imitating a perfect crystal at the lattice temperature of 0 K, *i.e.* when all other atoms were initially at their lattice positions and had zero initial velocities. This poses an important question of the effect of lattice temperature and the crystal size on the robustness of DBs, since all significant radiation effects are observed at temperatures above 300 K. In this relation, Zhang and Douglas [35] investigated interfacial dynamics of Ni nanoparticles at elevated temperatures exceeding 1000 K and discovered a string-like collective motion of surface atoms with energies in the eV range, *i.e.* exceeding the average lattice temperature by an order of magnitude. One of the most intriguing observations of this study was the propagation of the breather excitations along the strings, which demonstrates the robustness of

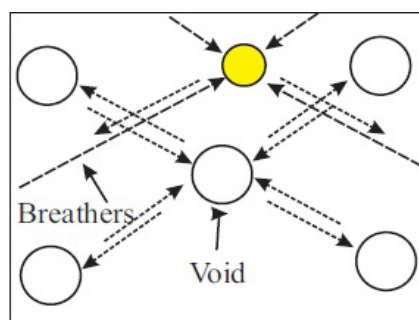


Fig. 10. Illustration of the dissolution of a void in the “interstitial” position due to the absorption of DBs coming from larger distances as compared to “locally ordered” voids that shield each other from the DB fluxes along the close packed directions [34]³.

DBs at elevated temperatures and shows the need of further investigations in this area.

References

1. S. R. MacEwen, G.J.C. Carpenter. *J. Nucl. Mater.* **90**, 108 (1980).
2. G.J.C. Carpenter, R.H. Zee, A. Rogerson. *J. Nucl. Mater.* **159**, 86 (1988).
3. V. Fidleris. *J. Nucl. Mater.* **159**, 22 (1988).
4. C.H. Woo. *Rad. Effects and Defects in Solids.* **144**, 145 (1998).
5. S.I. Golubov, A.V. Barashev, R.E. Stoller. On the origin of radiation growth of *hcp* crystals. ORNL/TM-2011/473.
6. G.D. Samolyuk, A.V. Barashev, S.I. Golubov, Y.N. Osetsky, R.E. Stoller. *Acta Materialia.* **78**, 173 (2014).
7. M. Griffiths. *J. Nucl. Mater.* **159**, 190 (1988).
8. S. Flach, A.V. Gorbach. *Phys. Rep.* **467**, 1 (2008).
9. M.E. Manley. *Acta Materialia.* **58**, 2926 (2010).
10. L.Z. Khadeeva, S.V. Dmitriev. *Phys. Rev.* **B81**, 214306 (2010).
11. A.A. Kistanov, S.V. Dmitriev. *Phys. Solid State.* **54**, 1648 (2012).
12. N.K. Voulgarakis, G. Hadjisavvas, P.C. Kelires, G.P. Tsironis. *Phys. Rev.* **B69**, 113201 (2004).
13. M. Haas, V. Hizhnyakov, A. Shelkan, M. Klopov. A. J. Sievers. *Phys. Rev.* **B84**, 14430 (2011).
14. A.V. Hizhnyakov, M. Haas, A. Pishtshev, A. Shelkan, M. Klopov. *Nucl. Instrum. Meth.* **B303**, 91 (2013).
15. A.V. Hizhnyakov, M. Haas, A. Pishtshev, A. Shelkan, M. Klopov. *Phys. Scr.* **89**, 044003 (2014).
16. A.A. Kistanov, R.T. Murzaev, S.V. Dmitriev, V.I. Dubinko, V. Hizhnyakov. *JETP Lett.* **99**, 353 (2014).
17. A.A. Kistanov, S.V. Dmitriev, A.S. Semenov A.S., V.I. Dubinko, D.A. Terent'ev. *Tech. Phys. Lett.* **40**, 657 (2014).
18. A. A. Kistanov, S. V. Dmitriev, A. P. Chetverikov, M. G. Velarde. *Eur. Phys. J.* **B87**, 211 (2014).
19. A. A. Kistanov, A.S. Semenov, R.T. Murzaev, S. V. Dmitriev. *Fundamentalnie Problemi Sovremennogo*

³ Note that similar to *hcp* metals, the void ordering in cubic metals has been observed both under neutron and electron irradiation [33], contrary to the statements made in Ref.[5].

- Materialovedeniya. **11**, 572 (2014).
20. A. A. Kistanov, R.T. Murzaev, S.V. Dmitriev, V.I. Dubinko, V. Hizhnyakov. JETP Lett. **99**, 403 (2014).
 21. V. I. Dubinko, Radiat. Eff. and Defects in Solids. **160**, 85 (2005).
 22. V.I. Dubinko. Radiation damage and recovery of crystals: Frenkel vs. Schottky defect production. In: Nuclear Materials, Editor: Michael P. Hemsworth, Nova Science Publishers, Inc. (2011).
 23. V. I. Dubinko, S. Hu, Yu Li, C. H. Henager, Jr., R.J. Kurtz. Philos. Mag. **92**, 4113 (2012).
 24. V.I. Dubinko, F.M. Russell. J. Nuclear Materials. **419**, 378 (2011).
 25. V. I. Dubinko, P. A. Selyshchev, J. F. R. Archilla. Phys. Rev. **E83**, 4 (2011).
 26. V.I. Dubinko. DCDS-S. **4**, 1119 (2011).
 27. V. I. Dubinko, A. V. Dubinko. Nuclear Inst. and Methods in Physics Research. **B303**, 133 (2013).
 28. V. Dubinko, R. Shapovalov. Theory of a quodon gas. With application to precipitation kinetics in solids under irradiation, Springer Int. Publ., Switzerland (2014).
 29. V. Dubinko, F. Piazza. On the role of disorder in catalysis driven by discrete breathers. Letters on Materials. **4(4)**, 273 (2014).
 30. M. A. Meyers, K.K. Chawla, Mechanical Behavior of Materials: Prentice-Hall. (1999) 555 p.
 31. V. I. Dubinko, A. S. Abyzov, A. A. Turkin. J. Nucl. Materials. **336**, 11 (2005).
 32. V.I. Dubinko, A. A. Turkin, A. S. Abyzov, M. Griffiths. Journal of ASTM Int. **3**, 157 (2006).
 33. Y. de Carlan, C. Regnard, M. Griffiths, D. Gilbon, C. Lemaignan, ASTM STP. **1295**, 638 (1996).
 34. K. Krihsan. Radiat. Eff. **66**, 121 (1982).
 35. S.B. Fisher, K.R. Williams. Radiat. Eff. **32**, 123 (1977).
 36. V. Dubinko. Nucl. Instrum. Meth. **B267**, 2976 (2009).
 37. H. Zhang, J. F. Douglas. Soft Matter. **9**, 1266 (2013).